JOURNAL OF CATALYSIS **159,** 112–118 (1996)
ARTICLE NO. 0070

CO, NO, and H_2 Adsorption on Ceria-Supported Pd

H. Cordatos and R. J. Gorte

Department of Chemical Engineering, University of Pennsylvania, Philadelphia, Pennsylvania 19104

Received August 18, 1995; revised October 30, 1995; accepted October 31, 1995

We have examined the adsorption of CO, NO, and H_2 on model Pd/ceria catalysts, formed by vapor deposition of Pd metal onto a flat, polycrystalline ceria support, using temperature programmed desorption. For CO adsorption on freshly deposited Pd films, a substantial fraction of the CO reacts to CO_2 in TPD, between 450 and 550 K, indicating that oxygen from ceria can react with CO on Pd. Prereduction of the catalyst by heating in CO or H_2 results in TPD curves which are virtually identical to that observed for Pd/α-Al_2O_3(0001), suggesting that electronic interactions between ceria and Pd have a negligible effect on the adsorption properties. For NO, there are differences between Pd/ceria and Pd/α-Al_2O_3(0001). A significantly higher fraction of the NO on Pd/ceria reacts to N_2 and N_2O, and prereduction of the Pd/ceria increases the amount of NO that can adsorb. Both of these results are interpreted as indicating that NO can adsorb on reduced ceria sites which are formed when lattice oxygen at the Pd-ceria interface is transferred to the Pd. For H_2, the desorption curves are similar to that observed on Pd/α-Al_2O_3(0001), except that the low-temperature feature assigned to the bulk hydride is less well resolved. If water is formed upon H_2 adsorption, it apparently readsorbs on the ceria. The implications of these results for reactions involving NO and CO on Pd/ceria are discussed. © 1996 Academic Press, Inc.

INTRODUCTION

Ceria-supported group VIII metals have received considerable attention in recent years, mainly due to their applications in automotive emissions-control catalysis. Ceria is added to automotive catalysts primarily for its oxygen-storage properties, which result from this oxide's ability to cycle between CeO_2 and CeO_{2-x}. However, many questions remain about the nature of interactions between ceria and catalytic metals and there are indications that Pt, Rh, and Pd do not all interact in the same manner with ceria. For example, in at least one catalyst formulation reported in the patent literature (1), it appears that an attempt was made to limit contact between Rh and ceria and maintain contact between Pt and ceria. Furthermore, Rh forms stable perovskites, while Pt and Pd do not (2). Differences were also reported from our laboratory on the oxygen transfer between ceria and supported Pt and Rh (3, 4), although more recent results have shown that this difference could have been due to the ceria structure (5).

In order to address the issue of possible differences between ceria-supported Pt, Rh, and Pd, we compare here the adsorption properties for CO, NO, and H_2 on ceria-supported Pd, Rh, and Pt using a series of model catalysts prepared under UHV conditions. Previous studies have demonstrated that adsorption properties on model catalysts of this type can be related to catalytic rates measured under steady-state conditions. For example, changes with particle size in the desorption kinetics of NO from Rh on model catalysts (6) can be related to changes in the steady-state NO reduction rates observed on high-surface-area catalysts (7). Similarly, changes in desorption kinetics of CO from Pt with particle size could be related to observations of steady-state CO oxidation rates (8, 9). Finally, TPD studies of model Rh–ceria catalysts, prepared using similar conditions to those in the present study, exhibited a ceria-mediated CO oxidation process (3, 10) which is also observable on high-surface-area catalysts (11).

Our present results demonstrate that CO adsorbed on Pd can react with oxygen from the ceria framework to form CO_2 in the same manner reported for Rh on ceria. With this exception, the desorption features for CO are otherwise very similar to that found for Pd on α-Al_2O_3(0001) (12), suggesting that the Pd itself is not strongly affected. For NO, we observe significantly more dissociation than was found for Pd/α-Al_2O_3(0001). Also, for reduced ceria, some of the NO adsorbs and dissociates on the ceria itself, as demonstrated by the significant increase in the adsorption uptakes. The implications of these results in automotive catalysts will be discussed.

EXPERIMENTAL PROCEDURE

Since the pretreatment and preparation conditions used for ceria can strongly affect the final properties (5), all of the experiments were performed on the same substrate. This substrate was prepared by spray pyrolysis of a 0.3-N aqueous solution of $Ce(NO_3)_3$ (99.5% purity, Johnson Matthey) on an α-Al_2O_3(0001) single crystal, using an N_2 carrier gas, while holding the sapphire crystal at ~650 K. After ceria deposition, the sample was placed in an oven and held at ~900 K, in air for 2 hr. This procedure was repeated three times to produce a final ceria film ~20 μm

0021-9517/96 $18.00
Copyright © 1996 by Academic Press, Inc.
All rights of reproduction in any form reserved.

thick. Finally, the sample was heated overnight at 970 K, a temperature at least 250 K higher than the decomposition temperature of $Ce(NO_3)_3$ (13).

A complete description of the films is given elsewhere (5). Briefly, X-ray diffraction patterns of films prepared using the same procedure demonstrated that the sample had the CeO_2 fluorite structure. Using Scherrer's formula for the line-broadening of the peak at 28.4°, we estimated the ceria crystallite size to be ~9–12 nm. Scanning electron micrographs showed that the films were relatively flat, with cracks or fissures separating irregularly shaped islands of ~1μm in size. The surface area was found from BET measurements to be 12 m^2/g. If one assumes that the ceria consists of dense, spherical particles, this surface area would be obtained for particles 0.1 μm in diameter, which implies there must be some porosity in the islands.

The UHV chamber used for the TPD measurements has a base pressure of $\sim 4 \times 10^{-10}$ Torr. It is equipped with a cylindrical mirror analyzer for Auger electron spectroscopy (AES) and a quadrupole mass spectrometer, interfaced with a computer for data acquisition and multiplexing. To improve sensitivity and baselines of the TPD, the quadrupole was placed inside a stainless-steel cone with an aperture, in front of which the sample could be placed. The oxide substrate was mounted on a Ta foil that could be cooled to 120 K or heated resistively to 900 K. A chromel-alumel thermocouple, attached to the back side of the α-Al_2O_3 crystal via a ceramic adhesive, was used to monitor the temperature. The adsorbates were introduced to the chamber through two beam dosers in order to maintain a low base pressure. The pressure in front of the doser has been estimated to be approximately 20 times higher than the background pressure, and exposures quoted in this manuscript were determined using this factor.

The ceria substrate was cleaned by ion bombardment at 500 K to remove all impurities observable by AES, followed by annealing in 1×10^{-7} Torr O_2 at 900 K for 30 min. The final oxidation-step involved cooling the sample to 400 K in 1×10^{-7} Torr O_2. Following evacuation, the noble metals were deposited at room temperature. The model catalysts at this stage will be referred to as "fresh." The AES peak intensities for Pd as a function of metal coverage were very similar to those reported for Pd/α-Al_2O_3(0001), suggesting that the growth of the metal film was nearly two-dimensional (12). Simply heating the samples above 650 K resulted in an irreversible, decreased peak intensity for Pd in AES, along with an increased intensity for oxygen, indicating that the metal film coalesced into particles at this temperature. Heating the samples in 1×10^{-7} Torr CO or H_2 for 10 min at 650 K, followed by briefly heating to 800 K in vacuum, induced changes in the desorption curves. Samples pretreated in this manner will be referred to as "reduced". For most of the experiments in this study, CO was used as the reductanct.

For CO and ^{15}NO, adsorption was performed at room temperature, while H_2 was adsorbed at 120 K. Typical exposures were approximately 10 L (1 Langmuir = 10^{-6} Torr · sec = 3.7×10^{14} molecules/cm^2 for NO at 300 K), which were sufficient to achieve saturation. For all TPD measurements, the heating rate was 10 K/sec. After each NO TPD, oxygen resulting from dissociation was removed by exposing the sample to CO and heating to 700 K. The desorption rates, r_d, in each figure are in arbitrary units, but all curves are drawn to the same scale.

RESULTS

CO Adsorption on Pd/CeO_2

The TPD curve following a saturation exposure of the as-deposited, fresh, 5×10^{15}Pd/cm^2 film to CO is shown in Fig. 1a. It is very similar to curves obtained from Pd particles on α-Al_2O_3(0001) (12), with the exception that a significant amount, ~20%, of the CO reacts to CO_2 between 450 and 550 K. The CO peak exhibits a single maximum at 490 K and a low-temperature shoulder at ~370 K, similar to what is observed for CO from Pd single crystals (14). These desorption features have previously been assigned to CO which is bridge bonded and terminally bonded, respectively (15). The source of the oxygen needed to form CO_2 appears to be the ceria. The Pd was not exposed to

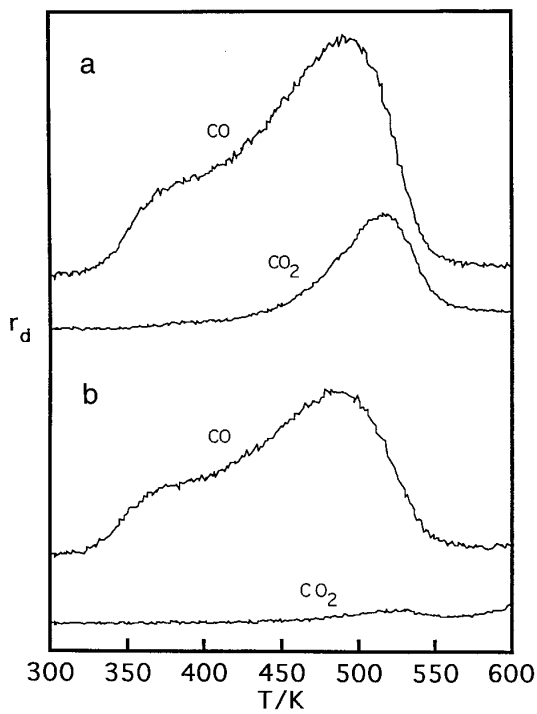

FIG. 1. Saturation TPD curves following CO adsorption at room temperature on a film of 5×10^{15} Pd/cm^2 (a) as deposited on ceria (fresh) and (b) after mild reduction in CO (reduced).

oxygen prior to the adsorption of CO; furthermore, if the CO_2 was the product of coadsorbed oxygen, it would appear in a peak centered at a lower temperature (16). We found no evidence for carbon deposition from either AES or subsequent TPD curves; therefore, the oxygen is not the result of CO dissociation. Rather, the results for Pd/ceria are very similar to those reported for Rh/ceria (3), where reduction of the ceria is the source of the oxygen.

After heating the film to 700 K during this first TPD measurement, the Pd film coalesced into larger particles, as shown by AES. Subsequent TPD curves for CO were very similar to that shown in Fig. 1a. Except that the amount of CO_2 decreased monotonically, similar to what has been reported for Rh/ceria (3). After the film had coalesced into particles, the sum of the CO and CO_2 peaks remained approximately constant, indicating that the size of the particles did not change substantially following the first annealing cycle. Using the sum of he CO and CO_2 areas in TPD to determine the dispersion and to calculate a particle size, as described elsewhere (17), we estimate the average Pd particle diameter to be ~9 nm. The CO TPD curve on the reduced sample, obtained after heating it in CO at 650 K, is shown in Fig. 1b. There is no significant change in the desorption features for CO, but the amount of CO_2 formed is now negligible. Annealing to 950 K in vacuum restored some of the ability of the surface to oxidize CO, as reported previously for Rh/ceria (3), indicating that oxygen could be brought out from the bulk of the ceria.

In order to investigate the effect of Pd particle size, the same adsorption measurements were performed on a film with 1×10^{15} Pd/cm^2. The TPD curves are not shown because they are so similar to those obtained for 5×10^{15} Pd/cm^2. The minor differences were as follows: First, the fraction of the CO which reacted to CO_2 in TPD was higher and CO_2 formation appeared to start at slightly lower temperatures. For example, the first TPD curve on the fresh film gave a CO_2 peak area which was 30% of the CO peak area. The increased fraction of CO reacting to CO_2 is consistent with oxygen originating at the edge of the metal crystallites, as suggested in recent reaction measurements (18). Second, the particle size determined after annealing this sample to 700 K, again determined by CO adsorption capacity, was found to be 5.2 nm, which is smaller than that obtained for larger metal coverages and consistent with that found for similar metal coverages on α-Al_2O_3(0001) (12). There is no evidence for CO adsorption on either oxidized or reduced ceria. Finally, a higher fraction of the CO on the reduced sample desorbed in the 370 K peak for the lower Pd coverage, consistent with the smaller Pd particle size.

NO Adsorption on Pd/CeO_2

In order to examine the role of ceria in the adsorption and dissociation of NO on Pd, we compare the TPD curves for Pd/ceria with those for Pd/α-Al_2O_3(0001) (12). Since the TPD curves for NO on Pd/α-Al_2O_3(0001) were virtually identical to those obtained for Pd on amorphous silica (19), we suggest that the sapphire support is noninteracting and that the results on this surface simply represent the desorption of NO on small Pd particles. Figures 2 and 3 show the desorption results for NO from the fresh and reduced Pd films of 5 and 1×10^{15} Pd/cm^2, respectively, with the analogous results for the same metal coverages on the sapphire crystal in the upper right corner. The results on α-Al_2O_3(0001) were obtained after heating the films to 700 K to form particles. To remove oxygen formed by NO dissociation, CO was adsorbed and the sample flashed to 700 K between NO TPD measurements. ^{15}NO was used in all of the experiments to eliminate any ambiguity in determining the products.

For 5×10^{15} Pd/cm^2, most of the NO desorbs unreacted for the sapphire substrate, as shown in Fig. 2. For Pd/ceria, however, only a small fraction of the NO desorbs intact on both the fresh and reduced surfaces. The TPD curves

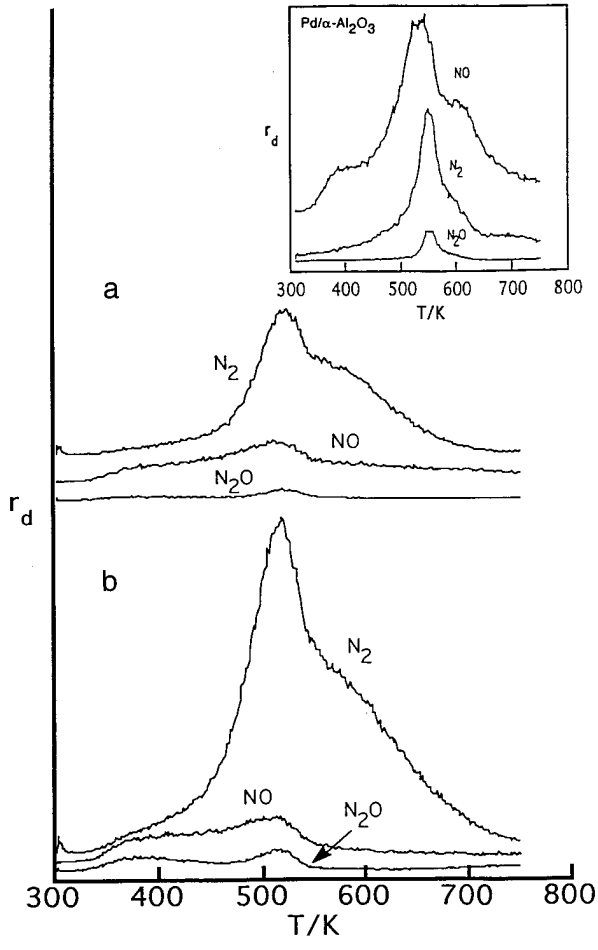

FIG. 2. TPD curves following NO adsorption at room temperature on (a) a fresh and (b) a reduced film of 5×10^{15} Pd/cm^2 on ceria. The NO TPD curves obtained from a Pd/α-Al_2O_3 film with the same Pd loading, taken from reference (12), are shown in the insert at the top right of the figure.

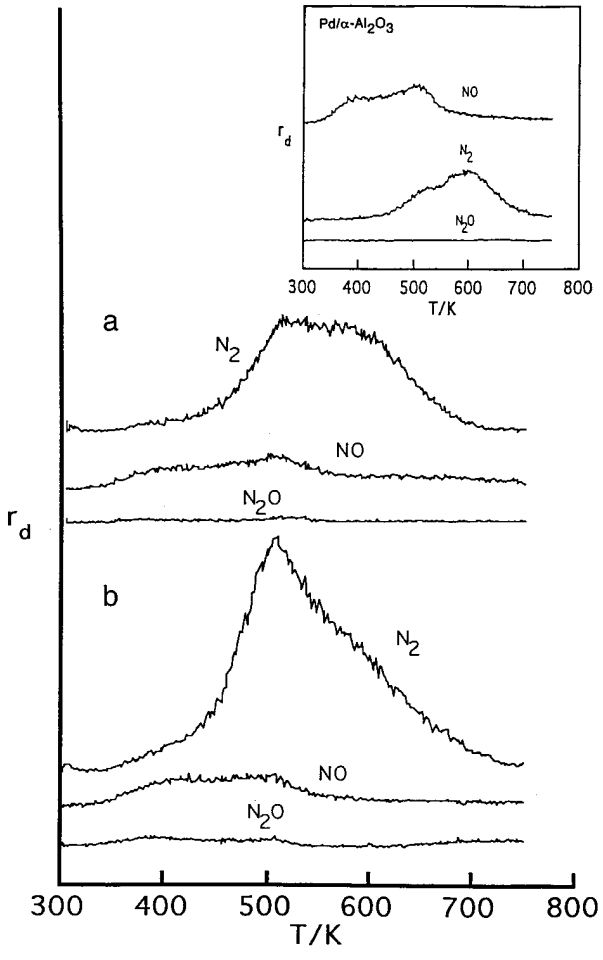

FIG. 3. TPD curves following NO adsorption at room temperature on (a) a fresh and (b) a reduced 1×10^{15} Pd/cm^2 film on ceria. The NO TPD curves obtained from a Pd/α-Al_2O_3 film of the same film loading, taken from reference (12), are shown in the insert at the top right of the figure.

on Pd/ceria are qualitatively similar, independent of pretreatment, showing unreacted NO in a peak centered at 510 K, with a leading shoulder extending to 350 K. The main desorption product is N_2, which desorbs in a narrow feature at 510 K and a second, overlapping, broad feature at ~590 K. A small amount of N_2O is also observed in peaks at 390 and 510 K. The effect of reducing the Pd/ceria was to dramatically increase the amount of N_2 formed and to increase slightly the N_2O, while not changing the molecular NO peak. The simultaneous desorption of NO, N_2 and N_2O at 510 to 550 K on both Pd/ceria and Pd/alumina suggests that some surface processes remain unchanged, but the relative amounts of each product are quite different.

The two important questions are (i) how does reducing the catalyst change the adsorption properties and (ii) how does ceria affect the decomposition of NO. We believe the answer to both these questions is that NO adsorbs on the reduced ceria, which is similar to what was previously reported for lanthana (20). First, we observed negligible adsorption on the ceria without Pd, demonstrating that the oxidized ceria cannot adsorb NO. The evidence that NO can adsorb on the reduced ceria comes from the total amounts of NO which adsorb. A reasonable estimate of the saturation coverages for NO can be obtained by summing the areas under the NO, N_2, and N_2O features and comparing these to the saturation CO coverage. For Pd/α-Al_2O_3(0001), this ratio was 0.7 (12). On the fresh and reduced Pd/ceria catalysts, these ratios were 0.8 and 3.5, respectively. Obviously, the large amount of NO on the reduced sample suggests that adsorption occurs on the ceria. NO reoxidizes CeO_{2-x} and desorbs as N_2. Adsorption on reduced ceria may also explain why more NO decomposes in TPD on the fresh sample. If Pd is oxidized and ceria reduced, either at room temperature or during the temperature ramp, NO could adsorb on the ceria. Coadsorption of NO and oxygen on Pd should certainly *decrease* the NO decomposition rate (21) and the CO results suggest that the Pd properties are not significantly changed, so that reaction on reduced ceria is the most reasonable explanation of the increased NO decomposition. The similarities in the desorption temperatures for both fresh and reduced Pd/ceria further agrees with this interpretation.

The TPD curves for 1×10^{15} Pd/cm^2 are qualitatively similar, as shown in Fig. 3. We again find that most of the NO dissociates to desorb as N_2 at the same temperatures observed for the higher Pd coverage, only the amounts are much less. Reducing the catalyst again increases the adsorption uptake. The sum of the peak areas for NO, N_2, and N_2O, ratioed to the CO and CO_2 areas, were 1.0 for Pd/α-Al_2O_3(0001), 0.9 for fresh Pd/ceria, and 2.0 for reduced Pd/ceria. Since the N_2 desorption features overlap with those observed on Pd/α-Al_2O_3(0001) at this Pd coverage, desorption from Pd could contribute to the features. We also observe a trace of N_2O on the Pd/ceria, which was not observed for Pd/sapphire, suggesting that the N_2O is formed on the oxide.

H_2 Adsorption on Pd/CeO_2

The TPD curves obtained following a saturation exposure of H_2 at 120 K to fresh Pd/ceria catalysts with Pd coverages of 5×10^{15} and 1×10^{15} Pd/cm^2 are given in Fig. 4, along with the corresponding TPD curve for 5×10^{15} Pd/cm^2 on α-Al_2O_3(0001). For Pd/α-Al_2O_3(0001), one observes a well-defined peak below 200 K for the larger particles, which is attributable to subsurface H_2 (12). This feature is not observed to any great extent on smaller Pd particles on α-Al_2O_3(0001). Surface hydrogen on Pd/α-Al_2O_3(0001) desorbs in a broad feature between 250 and 400 K, essentially independent of particle size. For the Pd/ceria samples, only molecular H_2, no water, desorbed in two broad peaks at 200 and 320 K. Except for the amount of H_2 which desorbed, both TPD profiles were essentially the same. While H_2 is

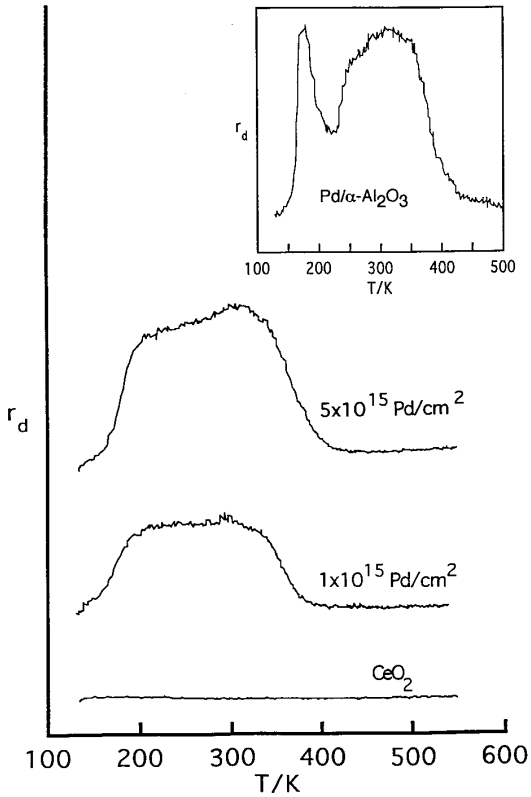

FIG. 4. TPD curves following H_2 adsorption at 120 K on pure ceria as well as for two different loadings of Pd on ceria (1 and 5×10^{15} Pd/cm^2). The TPD curve obtained from a 5×10^{15} Pd/cm^2 loading on α-Al_2O_3, taken from reference (12), is shown in the insert at the top right of the figure.

seen below 250 K, which might indicate subsurface species, the desorption feature is broad, unlike the alumina case.

The most interesting question regarding H_2 from Pd/ceria is why is water not observed in TPD. If the explanations for CO and NO adsorption on these catalysts are correct, that the Pd is oxidized by contact with the ceria, we should form water from the coadsorbed hydrogen and oxygen. As we discussed earlier, heating the samples in 1×10^{-7} Torr of H_2 for 10 min at 500 K was sufficient to reduce the sample so that adsorption of CO showed only CO in TPD. Therefore, we suggest that water simply readsorbs on the ceria and then either desorbs in a such a broad feature that it is lost in the baseline or is absorbed into the ceria bulk. (The presence of hydrogen in ceria has been discussed by others (28).) The conclusion that water is simply not observed in our TPD measurement was varified in coadsorption measurements with O_2 and H_2, in which the TPD curves were similar to those reported here and no water was seen.

Comparisons with Rh/CeO_2 and Pt/CeO_2

It is interesting to consider how specific the interactions are between ceria and the catalytic metal. Previously, it was reported that the properties of Pt and Rh particles on ceria were different in that CO on Rh/ceria resulted in CO_2 formation, while very little CO_2 was observed for Pt/ceria (3, 4). More recently, it was shown that Rh particles on CeO_2(111) and ceria films annealed at high temperatures do not exhibit CO_2 formation in TPD (22). The pretreatment conditions used for the ceria, therefore, appear to strongly affect the final properties of the catalyst. To do a fair comparison of Pt, Pd, and Rh on ceria, therefore, we examined the desorption of CO from each of the three metals deposited on the same ceria substrate, sputtering the sample clean between the deposition of each metal. The results for fresh Rh/ceria and Pt/ceria, with metal coverages of 1.5×10^{15}/cm^2, are shown in Figs. 5a and 5b.

The results for Rh/ceria are virtually identical to TPD curves reported earlier (3). CO desorbs at 490 K, with a shoulder to lower temperatures, similar to that observed on Rh single crystals. Substantial amounts of CO_2 are also formed, consistent with what would be expected for coadsorbed CO and oxygen. Contrary to previous reports, the results for Pt, Fig. 5b, also show significant CO_2 formation and could be consistent with coadsorbed CO and oxygen. For both Pt and Rh, reduction of the surfaces by heating in either CO or H_2 gave samples which exhibited CO TPD curves similar to that for Pt or Rh on alumina (23), with no evidence for CO_2 formation.

The previous results for Pt/ceria appear to be the result of high-temperature annealing of the ceria, which has

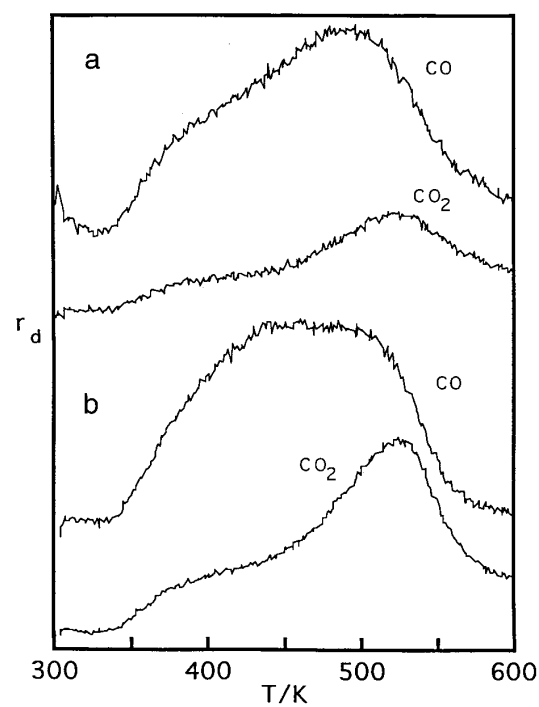

FIG. 5. TPD curves following CO adsorption at room temperature of a fresh film of (a) 1.5×10^{15} Rh/cm^2 and (b) 1.5×10^{15} Pt/cm^2 on ceria.

already been shown to cause deactivation (5). The NO desorption results reported in this earlier study of Pt/ceria were identical to results for Pt/alumina (24). If it were simply a question of the ceria having been reduced, that study should have observed enhanced N_2 formation and new desorption features, similar to what was observed in the present study on Pd/ceria. This further points out the importance of ceria structure in the adsorption properties of ceria-supported metals.

DISCUSSION

The central questions addressed in this paper are as follows: (i) What is the nature of support interactions between ceria and group VIII metals? (ii) How do the adsorption and reaction properties of group VIII metals supported on ceria differ from catalysts formed on alumina supports? Each of these issues will be addressed in turn.

First, the ability of CO on Pd, Pt, and Rh to react with lattice oxygen from ceria suggests that all three catalytic metals exhibit similar interactions with ceria. Since each of the metals have different stable oxidation states and form different compounds, interfacial compound formation would not appear to be necessary for the reaction to occur. It is possible that oxidation of CO occurs through a complex at the boundary between the metals and ceria, and evidence for these boundary states has been presented from IR spectra on lanthana-promoted Rh/SiO_2 (25). Since H_2 is equally effective at reducing ceria in our studies, a similar state would have to be invoked for hydrogen. However, it is our opinion that the best explanation for our results is that the metals are oxidized by the reduction of ceria since the TPD curves for CO are so similar to those observed when CO and oxygen are coadsorbed. While the redox process, $M + CeO_2 \rightarrow MO_x + Ce_2O_3$, is not thermodynamically favored for these catalytic metals based on bulk thermodynamic properties (3), there are a number of reasons the thermodynamic data for bulk materials may not be meaningful. First, it is known that CeO_2 can be reduced by as much as 17% without changing from the fluorite structure to the hexagonal Ce_2O_3 structure (29). Second, the observed sensitivity for CO_2 formation from Rh/ceria on ceria structure suggests that the properties of ceria in these nonannealed films are not the same as for bulk structures (5). Indeed, there is precedence for changes in the free energies of oxides like ceria with particle size in that high-pressure forms of ZrO_2 and Y_2O_3 can be stabilized at low pressures by forming small crystallites (26).

Electronic effects are often invoked to explain support effects, but these do not appear to be important for ceria. Following reduction of the ceria, which should maximize interactions based on most theories of support interactions, the desorption curves for CO from Pd/ceria are identical to those found for Pd on an inert substrate, α-$Al_2O_3(0001)$ (12). Similar results were found for Rh and Pt. Since desorption temperatures are a sensitive measure of the adsorption properties of the catalyst, changes in the metal properties should be reflected in the TPD curves. There is also no evidence for ceria migration onto the metals, such as has been reported for titania-supported metals (27).

The picture of ceria support effects that emerges, then, is one in which oxygen and possibly NO move relatively freely between the ceria and the catalytic metal. Lattice oxygen from CeO_2 at the metal–ceria boundary provides oxygen to the metal for oxidation reactions, while reduced sites at the boundary provide adsorption sites for NO. These reduced sites can be oxidized by NO, giving up N_2 and completing the oxidation–reduction cycle.

Regarding the adsorption and reaction properties of ceria-supported Pd, the TPD results show that there are significant changes due to the presence of ceria. For CO, obviously, the reaction with lattice oxygen from the ceria provides a second pathway for CO oxidation. Previous work with Rh/ceria has shown that this second pathway exhibits different reaction orders for both CO and O_2 from that observed for Rh/alumina under reducing conditions and also exhibits a lower activation energy (18). Therefore, the oxidation process observed in TPD influences the steady-state reaction rates, at least under some conditions. The results reported here for NO suggest that reactions of this molecule will also be strongly affected by the presence of ceria under net reducing conditions. The relatively free movement of molecules between sites on the catalytic metal and on the ceria provides a means for enhancing NO dissociation. This could be very important for metals like Pt and Pd which are not active for NO dissociation. Therefore, based on our TPD results, one would predict that the presence of ceria could significantly enhance NO reduction. Comparisons of rates for NO reduction by CO on Pd/alumina and Pd/ceria are presently being performed in our laboratory to test this prediction.

SUMMARY

The desorption measurements in this study indicate that the effect of ceria on Pd is very similar to that found for Rh and Pt. There is no evidence for electronic interactions which modify the adsorption properties of the metal, but it appears that lattice oxygen from the ceria can be transferred to the metal surface. This results in CO_2 formation at relatively low temperatures upon the adsorption of CO. The reduction of ceria by oxygen transfer also frees sites for NO adsorption, and NO decomposes readily on reduced ceria. This may provide an additional reaction pathway for NO decomposition.

ACKNOWLEDGMENTS

This work was supported by the NSF, MRL Program, Grant DMR 88-19885. Supplies and supplimentary support were obtained from the DOE, Basic Energy Sciences, Grant DE-FG03-85-13350.

REFERENCES

1. Joyner, R. W., "Zirconium in Catalysis: a Review of Current Scientific Literature" prepared for Magnesium Electron Ltd.
2. Tejuca, L. G., Fierro, J. L. G., and Tascon, J. M. D., *Adv. Catal.* **36**, 237 (1989).
3. Zafiris, G. S., and Gorte, R. J., *J. Catal.* **139**, 561 (1993).
4. Zafiris, G. S., and Gorte, R. J., *Surf. Sci.* **276**, 86 (1992).
5. Cordatos, H., Bunluesin, T., Stubenrauch, J., Vohs, J. M., and Gorte, R. J., *J. Phys. Chem.* in press.
6. Altman, E. I., and Gorte, R. J., *J. Catal.* **113**, 185 (1988).
7. Oh, S. H., and Eickel, C. C., *J. Catal.* **128**, 526 (1991).
8. Altman, E. I., and Gorte, R. J., *Surf. Sci.* **172**, 71 (1986).
9. Zafiris, G. S., and Gorte, R. J., *J. Catal.* **140**, 418 (1993).
10. Zafiris, G. S., and Gorte, R. J., *J. Catal.* **143**, 86 (1993).
11. Oh, S. H., and Eickel, C. C., *J. Catal.* **112**, 543 (1988).
12. Cordatos, H., Bunluesin, T., and Gorte, R. J., *Surf. Sci.* **323**, 219 (1995).
13. Wendlandt, W. W., *Anal. Chim. Acta* **15**, 435 (1956).
14. Engel, T., and Ertl, G., *Adv. Catal.* **28**, 1 (1979).
15. Van Hardeveld, R., and Hartog, F., *Adv. Catal.* **22**, 75 (1972).
16. Stuve, E. M., Madix, R. J., and Brundle, C. R., *Surf. Sci.* **146**, 155 (1984).
17. Roberts, S., and Gorte, R. J., *J. Chem. Phys.* **93**, 5337 (1990).
18. Bunluesin, T., Cordatos, H., and Gorte, R. J., *J. Catal.* **157**, 222 (1995).
19. Xu, X., and Goodman, W. D., *Catal. Lett.* **24.**, 31 (1994).
20. Cordatos, H., and Gorte, R. J., *Appl. Catal.* in press.
21. Schmick, H. D., and Wassmuth, H. W., *Surf. Sci.* **123**, 471 (1982).
22. Stubenrauch, J., and Vohs, J. M., *J. Catal.* in press.
23. Altman, E. I., and Gorte, R. J., *Surf. Sci.* **195**, 392 (1988).
24. Altman, E. I., and Gorte, R. J., *J. Phys. Chem.* **93**, 1993 (1989).
25. Underwood, R. P., and Bell, A. T., *J. Catal.* **109**, 61 (1988).
26. Scandan, G., Foster, C. M., Frase, H., Ali, M. N., Parker, J. C., and Hahn, H., *Nanostructured Mater.* **1**, 313 (1992).
27. Ko, C. S., and Gorte, R. J., *J. Catal.* **90**, 59 (1984).
28. Laachir, A., Perrichon, V., Badri, A., Lamotte, J., Catherine, E., Lavalley, J. C., El Fallah, J., Hilaire, L., le Normand, F., Quemere, E., Sauvion, G. N., and Touret, O., *J. Chem. Soc. Faraday Trans.* **87**, 1601 (1991).
29. Sanchez, M. G., and Gazquez, J. L., *J. Catal.* **104**, 120 (1987).